Published in final edited form as:
Neuroimage. 2011 February 1; 54(3): 1872–1880. doi:10.1016/j.neuroimage.2010.09.070.

A Web-based Brain Atlas of the Vervet Monkey, *Chlorocebus aethiops*

Roger P. Woods[a,b,c,*], **Scott C. Fears**[c,d], **Matthew J. Jorgensen**[e], **Lynn A. Fairbanks**[c,d], **Arthur W. Toga**[b,f], and **Nelson B. Freimer**[c,d]

[a]Ahmanson-Lovelace Brain Mapping Center, University of California, Los Angeles (UCLA), Los Angeles, California, USA 90095

[b]Department of Neurology, University of California, Los Angeles (UCLA), Los Angeles, California, USA 90095

[c]Center for Neurobehavioral Genetics, University of California, Los Angeles (UCLA), Los Angeles, California, USA 90095

[d]Department of Psychiatry and Biobehavioral Sciences, University of California, Los Angeles (UCLA), Los Angeles, California, USA 90095

[e]Department of Pathology, Section on Comparative Medicine, Wake Forest University School of Medicine, Winston-Salem, North Carolina, USA 27157

[f]Laboratory of Neuroimaging, University of California, Los Angeles (UCLA), Los Angeles, California 90095

Abstract

Vervet monkeys are a frequently studied animal model in neuroscience research. Although equally distantly related to humans, the ancestors of vervets diverged from those of macaques and baboons more than eleven million years ago, antedating the divergence of the ancestors of humans, chimpanzees and gorillas. To facilitate anatomic localization in the vervet brain, two linked on-line electronic atlases are described, one based on registered MRI scans from hundreds of vervets (http://www.loni.ucla.edu/Research/Atlases/Data/vervet/vervetmratlas/vervetmratlas.html) and the other based on a high-resolution cryomacrotome study of a single vervet (http://www.loni.ucla.edu/Research/Atlases/Data/vervet/vervetatlas/vervetatlas.html). The averaged MRI atlas is also available as a volume in Neuroimaging Informatics Technology Initiative format. In the cryomacrotome atlas, various sulcal and subcortical structures have been anatomically labeled and surface rendered views are provided along the primary planes of section. Both atlases simultaneously provide views in all three primary planes of section, rapid navigation by clicking on the displayed images, and stereotaxic coordinates in the averaged MRI atlas space.

[*]**Corresponding author** Roger P. Woods, M.D. Phone: 001 310 794-4057 Fax: 001 310 794-7406 rwoods@ucla.edu Mail: Ahmanson-Lovelace Brain Mapping Center 660 Charles E Young Drive South Los Angeles, CA 90095-7085.
(rwoods@ucla.edu)
(fears.scott@gmail.com)
(mjorgens@wfubmc.edu)
(LFairbanks@mednet.ucla.edu)
(arthur.toga@loni.ucla.edu)
(NFreimer@mednet.ucla.edu)

Despite the extended time period since their divergence, the major sulcal and subcortical landmarks in vervets are highly conserved relative to those described in macaques.

Keywords

brain atlas; vervet; Old World monkey; *Chlorocebus aethiops*; magnetic resonance imaging; cryomacrotome

1. Introduction

Chlorocebus aethiops, commonly referred to as the vervet monkey or the African green monkey, is an Old World monkey and a member of the Cercopithecinae subfamily. This subfamily also includes other terrestrial guenons, arboreal guenons, macaques, baboons, mangabeys and mandrills. The Cercopithecinae are thought to have diverged from the other Old World monkey subfamily, the Colobinae, approximately 14 million years ago (Stewart and Disotell, 1998) with guenons subsequently diverging from baboons, macaques, mangabeys and mandrills around 11.5 million years ago (Tosi et al., 2005). Members of the terrestrial guenon genus *Chlorocebus* were previously classified together with arboreal guenons as the single genus *Cercopithecus* (Grubb et al., 2003) but have recently been reclassified into their own separate genus (Groves, 2001; Tosi et al., 2003; Tosi et al., 2005; Xing et al., 2007). Molecular studies indicate that the arboreal and terrestrial guenons diverged about 8 million years ago (Tosi et al., 2005). All Old World monkeys are equally distantly related to humans and apes, having diverged from a common ancestor approximately 30 million years ago (Steiper and Young, 2006). The relationships between vervets and other Old World monkeys, apes and humans are shown in Figure 1.

Although some early monkey brain cytoarchitectonic work (e.g., that of Brodmann (1909) and of Vogt and Vogt (1919)) was based on guenons (most likely the arboreal guenon *Cercopithecus campbelli* according to von Bonin and Bailey (1947)), modern monkey brain atlases have typically been based on macaques. Aside from an anatomically labeled atlas published in 1981 by Contreras et al. and an electronic collection of mostly unlabeled Nissl stained slides described by Mikula et al. (2007) (accessible at http://brainmaps.org), we are unaware of any modern structural anatomic atlas of the genus *Chlorocebus* or any other arboreal guenon. The value of an anatomic brain atlas specific to this species is underscored by the fact that the vervet is a well established animal model (Carrlson, 2004) that has been used to study numerous brain disorders and traits. These include Parkinson's disease (Taylor et al., 1997; Campos-Romo et al., 2009), Alzheimer's disease (Lemere et al., 2004; Fainman et al., 2007), recovery from early brain injury (Burke et al., 2010), African sleeping sickness (Ouwe-Missi-Oukem-Boyer et al., 2006), aging related brain changes (Melega et al., 2007), fetal alcohol syndrome (Burke et al., 2009), alcoholism (Ervin et al., 1990; Mash et al., 1996), phencyclidine use (Jentsch et al., 1997), cocaine use (Jentsch et al., 2002), methamphetamine use (Melega et al., 2008), stress (Uno et al., 1989), eating disorders (Laćan et al., 2008), stereotypic behaviors (Hugo et al., 2003), impulsivity and aggression (Fairbanks et al., 2004b; James et al., 2007), novelty seeking (Bailey et al., 2007), separation anxiety (Marais et al., 2006), processing of vocalizations (Gil-da-Costa and Hauser, 2006), cerebrospinal fluid dopamine metabolite levels (Freimer et al., 2007) and brain size (Fears et al., 2009). Vervets are likely to account for an increasing proportion of non-human primate neuroscience studies in the future since macaques, the most commonly studied Old World monkey, are in short supply by virtue of their use in AIDS research (Carlsson et al., 2004). Vervets are abundant in Africa and on certain islands in the Caribbean as well as being available in breeding colonies in the United States and elsewhere. Relative to macaques, vervets pose less risk to humans as they are not infected with Cercopithecine herpesvirus 1,

a herpes virus endemic in macaque colonies that has a 70% mortality rate when contracted by humans (Elmore and Eberle, 2008).

We have recently completed magnetic resonance imaging (MRI) of a large number of vervets from the UCLA-VA/Wake Forest Vervet Research Colony (Fears et al., 2009) and have assembled these scans into an averaged vervet MRI atlas. We have registered a very high resolution cryomacrotome anatomic data set collected from one member of this colony (Rubins et al., 1999) to this atlas and have labeled various sulcal and subcortical landmarks in this anatomic data set on all three primary viewing planes. To facilitate interpretation of the MRI images, the atlases have been incorporated into two interlinked Web-based viewer applications that simultaneously display transverse, coronal and sagittal sections with updating of sections whenever the user clicks on the images. Rendered surface views along the primary image axes are also included. Menu selections can be used to navigate directly to labeled structures. Stereotaxic coordinates of the current location are displayed. The images, labels and coordinate axes can be rescaled to any size in the viewer since the application is based on Scalable Vector Graphics (SVG) (http://www.w3.org/Graphics/SVG/), a scalable format viewable in most modern web browsers. To facilitate registration of other imaging data into this atlas framework, the data volume that was used to create the averaged MRI atlas is also available for download. We describe here the construction of this resource, which should be useful in interpretation of brain anatomic or imaging datasets collected from vervet monkeys. Due to strong conservation of brain anatomic features across all Old World monkey species, this electronic resource may be a useful supplement in interpreting such data from other monkey species as well.

2. Materials and Methods

2.1 The Vervet Research Colony

The UCLA-VA/Wake Forest Vervet Research Colony was founded from 57 wild-caught animals trapped on the island of St. Kitts in the Caribbean between 1975 and 1985. Ancestors of these animals are believed to have been brought to St. Kitts from Africa in the 1600's. Morphometric and DNA evidence suggests that these animals originated in West Africa and that they are members of the subspecies *Chlorocebus aethiops sabaeus* (van der Kuyl et al., 1996). At UCLA, the animals were maintained in a naturalistic setting in matrilineal breeding groups. None of the animals studied had undergone any experimental manipulations expected to alter brain structure. At the time of this study, the colony was housed in the Los Angeles area; the colony has subsequently been relocated to Wake Forest University.

2.2 Data Collection and Processing

All MRI and cryomacrotome procedures were conducted in accordance with the UCLA Animal Research Committee and with the Animal Research Committee of the Department of Veterans Affairs Greater Los Angeles Healthcare System.

2.2.1 MRI Data—Animals were scanned using a mobile 1.5 Tesla Siemens (Erlangen, Germany) Symphony unit located on the colony grounds. All available animals more than two years of age (357 in total) were scanned. The scanning procedure has been previously described in detail elsewhere (Fears et al., 2009). Briefly, animals were anesthetized with intramuscular ketamine (15 mg/kg) prior to insertion of an intravenous catheter. They were subsequently treated with atropine (0.027 mg/kg) to minimize secretions prior to endotracheal intubation to protect the airway. Anesthesia was maintained with intravenous ketamine and midazolam. Eight or nine T1-weighted scans (TR 1900 msec,TE 4.38 msec, TI

1100 msec, flip angle 15 degrees) were obtained from each animal using a multi-channel human knee coil (Invivo, Orlando) as a receiver. Image resolution was 0.5 mm in all three axes. All animals tolerated the procedure well.

MRI images were converted from DICOM format to 16-bit Analyze 7.5 format using in-house software. The MRI scans from each animal were coregistered to one another and averaged using a rigid-body spatial transformation model with the Automated Image Registration (AIR 5.2.6) package (Woods et al., 1998a). Non-brain structures were removed using a combination of manual and automated methods and the resulting brain-only images were registered to the images of one arbitrarily chosen animal using an affine spatial transformation model with AIR 5.2.6 (Woods et al., 1998b). Using the resulting spatial transformations, an average affine target space was defined (Woods, 2003a) and each animal's averaged MRI scan was resampled into this space and averaged to create a new target atlas. The registration and resampling processes were repeated iteratively until the resulting target atlas had converged to an atlas visually indistinguishable from its precursor. This final target atlas was adjusted to align the averaged anterior and posterior commissures horizontally and to place the mid-sagittal plane in the midline. The original images from each animal were corrected for inhomogeneities (Likar et al., 2001) and were resampled into the final atlas space using chirp-z interpolation (Woods et al., 1998a) using the spatial transformations derived from the steps described above. Ten animals noted to have macroscopic brain abnormalities were excluded and the remaining 347 images were averaged; in the course of averaging, gamma correction was applied to the output volume to improve gray-white contrast in the final images. The apex of the anterior commissure was identified in the averaged MRI images and was used as the origin of a stereotaxic coordinate system.

The final averaged image volumes were separated into individual transverse, coronal and axial slices using AIR and then losslessly converted to Portable Network Graphic (PNG) format (http://www.w3.org/Graphics/PNG/) using the open source software package ImageMagick (http://www.imagemagick.org/script/index.php).

2.2.2 Cryomacrotome Data—An eight year old male vervet monkey was sacrificed with an overdose of pentobarbital. The head was removed, debrided and rapidly frozen in isopentane chilled with liquid nitrogen. The frozen head was blocked in distilled water for cryosectioning and placed with the rostral aspect of the head facing downward. The brain remained in the skull for sectioning, thereby minimizing shape distortions. The head was sectioned in the coronal plane in 50 μm increments using a heavy duty sledge cryomacrotome (PMV, Stockholm, Sweden) at a temperature of −25° C. The knife speed was 3.5 m/min, and the knife was tilted 5° from the horizontal. A digital camera (Digistat 1024) with a 50 mm lens was mounted to the setup with a constant source of illumination (8 lamps, Cuda filter optics) allowing images of the exposed coronal brain sections to be obtained. Twenty-four bit color pictures of the exposed brain were taken every 300 μm, producing a total of 229 images covering 6.87 cm along the anterior-posterior axis. The original images were 1024 by 1024 pixels and were subsequently downsampled to 512 by 512 pixels. A ruler placed on the block face demonstrated that the pixel sizes in each image were 150 μm after downsampling. Images were stored in the portable pixmap (ppm) file format, a non-compressed file format with 24 bits per pixel. All of the above procedures were completed in 1998 and a gray scale stereotaxic atlas without anatomic labels generated from this data set has been previously reported in abstract form (Rubins et al., 1999).

The ppm images were retrieved to create the atlas reported here. To check the three dimensional integrity of the data, the images were converted to 8-bit grayscale raw images using Adobe Photoshop (Adobe Systems, San Jose). The individual images were then

combined into a three dimensional volume in Analyze 7.5 format and reviewed using MultiTracer (Woods, 2003b) which allows the data to be viewed in three orthogonal planes of section. A single, large (several pixels) shift of the camera relative to the block face was identified partway through the data set. The two 2D grayscale images immediately before and after this shift were converted to Analyze format and registered using a 2D rigid-body transformation model using AIR 5.2.6. Applying the resulting transformation to correct all of the images after the shift resulted in an internally consistent reassembled three dimensional volume. This volume was then registered to the affine MRI atlas created by averaging the 347 normal MRI scans from the Vervet Research Colony. This registration was performed using AIR 5.2.6 using an affine spatial transformation model.

The color ppm images were then converted into the International Commission on Illumination (CIE) 1976 (L*,a*,b*) color space (CIELAB D50) using Adobe Photoshop and the resulting three 8-bit channels were each stored separately as 8-bit raw format images. This color model was selected instead of the usual red-green-blue model because it is designed to approximate human visual perception. Images were corrected for the shift identified in the gray scale images usng AIR 5.2.6 with chirp-z interpolation (Woods et al., 1998a). These corrected 2D images were then combined into three 8-bit Analyze 7.5 format images to create volumes representing the L*, a* and b* channels of the original images. Using the transformation obtained by registering the 8-bit grayscale volume to the vervet MRI atlas, each of the 8-bit color channels were resliced using chirp-z interpolation to match the MRI atlas, but with voxel sizes of 0.166 mm × 0.166 m × 0.166 mm rather than the 0.5 mm × 0.5 mm × 0.5 mm dimensions of the MRI atlas. The interpolated volumes were then separated independently along the transverse, coronal and sagittal axes to create raw format slices for each color channel for each plane of section. Using Adobe Photoshop, the resulting 2D images from the three color channels were recombined and converted to Joint Photographic Experts Group (JPEG) file interchange format (http://www.w3.org/Graphics/JPEG/) with high quality (Q=8) output settings.

To create a grayscale version of the final cryomacrome atlas, the resampled L*,a* and b* images were combined and converted to an 8-bit Analyze 7.5 format volume. The outer surface of the cerebral hemispheres was manually contoured in this volume using MultiTracer and the contours converted into a point cloud used to generate a mesh representing the cortical surface. Conversion of the point cloud to a mesh was performed using methods implemented in MeshLab (http://meshlab.sourceforge.net/). Specifically, the point cloud was subsampled to generate a uniformly distributed set of points (Cline et al., 2009) and the surface mesh generated using algebraic point set surface methods as described by Guennebaud et al., (2008). The resulting mesh was displayed and converted to JPEG format using the Laboratory of Neuroimaging ShapeViewer (http://www.loni.ucla.edu/Software/ShapeViewer).

2.3 Atlas Viewer Construction and Anatomic Labeling

Web-based scalable vector graphics (SVG) viewers for the MRI and cryomacrotome data were created using ECMAScript code to load the appropriate images and update coordinate locations in response to mouse clicks on any of three orthogonal planes of view. Using the web-based viewer, the cryomacrotome data set was carefully reviewed and the positions of anatomic labels of sulcal anatomy and gray and white matter structures were determined. Where possible, abbreviations used for anatomic structures were the same as those of the atlas of the rhesus macaque (*Macaca mulatta*) by Paxinos et al. (2009), and the rhesus atlas was used as a guide for identifying the anatomic landmarks in the vervet. Labels were checked in all three views to assure internal consistency. A total of 28 sulcal landmarks were identified; the landmarks are their abbreviations are listed in Table 1. Coordinates for labels were identified on key planes in the vervet atlas and coordinate locations for intervening

planes were interpolated using cubic splines and modified when necessary to maintain anatomic integrity. Only sulci in the right hemisphere were labeled; labels can also be turned off in the viewer to allow an unobstructed view of the underlying anatomy.

2.4 Defining Affine Transformations to Rhesus Macaque Atlases

To define an affine transformation for mapping from the vervet atlas space created here and the rhesus macaque atlas space of Paxinos et al. (2009), the MNI rhesus macaque atlas, which is based on T1-weighted MRI scans of seven normal adult rhesus macaques and which has a known relationship to the Paxinos atlas (Chakravarty et al., 2009) was downloaded from http://www.bic.mni.mcgill.ca/ServicesAtlases/Rhesus and converted to Analyze 7.5 format. Non-brain structures were removed manually using MultiTracer (Woods et al., 2003b) and registered using an affine spatial transformation model to a similarly processed version of the vervet atlas using AIR 5.2.6 (Woods et al., 1998b). All associated linear transformations were combined into a single affine transformation for mapping directly from the vervet atlas space to the Paxinos atlas.

To define an affine transformation for mapping from the vervet atlas space to the rhesus macaque atlas space of Saleem and Logothetis (2007), the 112RM-SL T1-weighted atlas, which was created by McLaren et al., (2009) from T1-weighted MRI scans of 112 rhesus macaques and which shares the coordinate system of the Saleem and Logothetis atlas, was downloaded from http://www.brainmap.wisc.edu/monkey.html and converted to Analyze 7.5 format. Non-brain tissues have already been removed from this atlas, which was registered to the vervet MRI atlas to generate a single affine transformation for mapping from vervet atlas space to the Saleem and Logothetis atlas as described above for the Paxinos atlas.

To verify the quality of the affine registrations mapping between the MRI atlases, the original MNI rhesus macaque MRI atlas and the original 112RM-SL T1-weighted atlas were resampled into the vervet MR atlas space using AIR 5.2.6. To facilitate comparison, contrast and brightness were adjusted in the latter two atlases to approximate that of the vervet MRI atlas.

3. Results

The averaged MRI atlas is available at http://www.loni.ucla.edu/Research/Atlases/Data/vervet/vervetmratlas/vervetmratlas.html, and the corresponding anatomically-labeled cryomacrotome atlas is available at http://www.loni.ucla.edu/Research/Atlases/Data/vervet/vervetatlas/vervetatlas.html. Corresponding views from the cryomacrotome and averaged MRI atlases are shown in Figures 2–4. Support for SVG 1.1 (http://www.w3.org/TR/SVG11/) is needed to view the atlases; the Mozilla Firefox browser (www.mozilla.org) has a native implementation of SVG 1.1 and is the recommended browser since it supports all implemented atlas features and has been extensively tested during development. All major modern web browsers except Microsoft's Internet Explorer currently have native SVG support, but bugs and incomplete implementations may render some atlas features inoperable in some browsers. Native SVG support is expected in the next release of Internet Explorer.

The averaged MRI atlas in the Neuroimaging Informatics Technology Initiative (NIfTI-1.1) format is also available via the “Download” link at http://www.loni.ucla.edu/Atlases/Atlas_Detail.jsp?atlas_id=21.

The overall registration between the two atlases is good, allowing features in the unlabeled MRI atlas to be readily identified by reference to the labeled high resolution cryomacrotome

data set. In most regions, misregistration is less than one millimeter. Discrepancies are somewhat larger posteriorly near the ventricles and near the junction of the lateral and superior temporal sulci where misregistrations up to 2.5 millimeters can be seen. It is likely that this relates in part to non-linear post-mortem changes not correctable by affine registration. For example, the posterior commissure is displaced inferiorly in the cryomacrotome atlas, collapsing the Sylvian aqueduct, which is readily seen in its uncollapsed state in the MRI atlas.

From the standpoint of comparative anatomy, we were able to identify in the cryomacrotome data set all of the major sulci shown in the rhesus macaque atlas of Paxinos et al. (2009) with the exception of the superior parietal sulcus, a shallow sulcus found on the mesial surface of the macaque brain, and the ectocalcarine sulcus, a shallow sulcus on the convexity of the occipital lobe. Figure 5 shows sagittal sections of the vervet MR atlas, the MNI rhesus macaque MRI atlas (Chakravarty et al., 2009) and the 112RM-SL T1-weighted rhesus macaque MRI atlas of McLaren et al. (2009) as registered in the framework of the vervet MR atlas. Small differences are apparent, but the overall registration of homologous macroscopic landmarks is good.

3.1 Transformations to and from the Paxinos Rhesus Atlas

Paxinos et al (2009) do not explicitly state whether the right hemisphere or left hemisphere was used to generate the stained sections illustrated and labeled in their atlas. Implicitly, Chakravarty et al. (2009) treat the sections as coming from the right hemisphere, a convention adopted here as well. Defining F as the figure position (increasing anteriorly), L as the distance from midline (increasing to the right) and S as the distance along the inferior/superior axis defined by the left sided ruler in the Paxinos atlas (increasing superiorly) and X, Y and Z as millimeter coordinates relative to the MRI anterior commissure in the vervet atlas, the following transformations apply:

$$X = 0.87376*L - 0.01201*F - 0.01834*S - 1.48889$$

$$Y = 0.08898*L + 0.89092*F - 0.15981*S + 4.11279$$

$$Z = -0.01796*L + 0.08604*F + 0.84111*S - 13.16340$$

$$L = 1.14374*X + 0.01277*Y + 0.02736*Z + 2.01057$$

$$F = -0.10787*X + 1.10101*Y + 0.20684*Z - 1.96611$$

$$S = 0.03545*X - 0.11236*Y + 1.16833*Z + 15.89401$$

Since nonlinear discrepancies are present between the vervet cryomacrotome atlas and the vervet MRI atlas and likewise between the MNI rhesus macaque atlas and the atlas of Paxinos et al. (2009) (Chakravarty et al., 2009), the mapping provided by these equations is only approximate; further refinement based on inspection of local anatomic features is recommended.

3.2 Transformations to and from the Saleem and Logothetis Rhesus Atlas

Defining X1, Y1 and Z1 as millimeter coordinates relative to the interaural line in the Saleem and Logothetis rhesus atlas and X,Y and Z as millimeter coordinates relative to the MRI anterior commissure in the vervet atlas, the following transformations apply:

$$X = -0.89422*X1 - 0.01773*Y1 + 0.00734*Z1 - 0.52123$$

$$Y = -0.01526*X1 + 0.85748*Y1 - 0.09636*Z1 - 17.15442$$

$$Z = 0.00142*X1 + 0.13215*Y1 + 0.84773*Z1 - 13.52061$$

$$X1 = -1.11787*X - 0.02418*Y + 0.00692*Z - 0.90388$$

$$Y1 = -0.01935*X + 1.14571*Y + 0.13039*Z + 21.40690$$

$$Z1 = 0.00489*X - 0.17857*Y + 1.15929*Z + 12.61358$$

As with the Paxinos Rhesus Atlas, refinement based on inspection of local anatomic features is recommended to compensate for nonlinear discrepancies not captured by these affine transformations.

4. Discussion

Brain atlases have evolved considerably in recent years. Older two-dimensional atlases were based on hand sectioned slices that were photographed and labeled in printed form. Such atlases were typically based on a single animal and did not attempt to capture the variability from one animal to another. The advent of high resolution cryomacrotome imaging now allows data from a single animal to be digitally resectioned and formatted in a three dimensional context (Cannestra et al., 1997; Annese and Toga, 2002), which has led to the production of very high quality printed stereotaxic atlases (e.g., Saleem and Logothetis, 2007; Paxinos et al., 2009). Nonetheless, we are not aware of any openly accessible digital non-human primate atlas that provides all of the dynamic interactive features of the labeled cryomacrotome atlas described here. Averaged MRI atlases have found widespread use in the context of human brain mapping studies (Mazziotta et al., 2001), and averaged T1-weighted MRI atlases have been previously described for the baboon (*Papio anubis*) (Black et al., 2001a; Greer et al., 2002), the pig-tailed macaque (*Macaca nemestrina*) (Black et al., 2001b), the long-tailed macaque (*Macaca fascicularis*) (Black et al., 2005) and the rhesus macaque (*Macaca mulatta*) (McLaren et al., 2009). As with human data, these atlases can be used as species-specific registration targets for combining imaging data obtained through MRI or positron emission tomography. The associated cryomacrotome atlas described here provides efficient access to anatomic features visible in the MRI data.

It has long been known that major sulcal and gyral patterns are widely preserved across Old World monkey species (Connolly, 1936), with minor sulci showing a greater degree of variability (Connolly, 1936; Van Der Gucht et al., 2006). The most substantial reported anatomic differences are those between the Cercopithecinae and the Colobinae (Falk, 1978), the most ancient subdivision of Old World monkeys, but even in that case, the overall pattern of sulci and gyri is quite similar. As shown in Figure 5, simple affine transformations can account for most of the differences between vervets and rhesus macaques, but differences remain that would require nonlinear deformations for precise matching of macroscopic landmarks. This is not surprising given that such differences have been reported even between different macaque species (McLaren et al., 2009) and underscores the relevance of species specific atlases. The preservation of sulcal and gyral anatomic patterns for the 11.5 million years since divergence of vervets and macaques contrasts sharply with the anatomic differences that developed between chimpanzees and humans over six to seven million years.

Although von Bonin and Bailey (1947) specifically commented on the cytoarchitectonic similarity between *Macaca mulatta* and *Cercopithecus campbelli* (an arboreal guenon more closely related to *Chlorocebus aethiops* than to macaques or baboons), we have not attempted to extrapolate cytoarchitectonic data from other species into the vervet atlas. Arboreal guenons are the monkeys most closely related to the vervet for which extensive cytoarchitectonic data are available (Brodmann, 1909; Vogt and Vogt, 1919), but the hypothesis that *Chlorocebus aethiops* is cytoarchitectonically closely similar to arboreal guenons after eight million years of divergence is untested. Even greater concern in extrapolating vervet cytoarchitectonics from macaque cytoarchitectonics is underscored by the fact that the prelunate gyrus of the terrestrial guenon *Erythrocebus patas* shows certain

cytoarchitectonic features distinct from those seen in macaques (Van Der Gucht et al., 2006); other brain regions were not included in this analysis. Future direct cytoarchitectonic studies in *Chlorocebus aethiops* will be needed to provide definitive cytoarchitectonic information that can be used with confidence. In the interim, the coordinate transformations into the rhesus macaque atlases of Saleem and Logothetis (2007) and of Paxinos et al. (2009) provide a provisional starting point for estimating vervet cytoarchitectonics.

While specialized imaging tools to display anatomic images three-dimensionally have been freely available for several years (e.g., Woods et al., 2003b), the recent implementation of SVG viewing capabilities in most modern web browsers now greatly simplifies the task of making such information, together with anatomic labels, readily available on the internet without the need for specialized browser plug-ins. The ability to localize a position simultaneously in three different planes of section provides much greater insight into anatomic structure than individual slices in a single plane of section. To encourage the development of publicly available atlases in this format, all of the images in the atlases and the markup used to display them are freely available for reuse and redistribution under the terms of the Creative Commons Attribution License (http://creativecommons.org/licenses/by/3.0/). External links into the atlases can be configured to direct users to a specific set of slices in the atlas by including the X, Y and Z coordinates in the URL. For example, an external link to http://www.loni.ucla.edu/Research/Atlases/Data/vervet/vervetatlas/vervetatlas.html?X=370&Y=271&Z=163 will load the cryomacrotome images setting the view and crosshairs to display the hippocampus.

The primary long term objective in collecting the MRI data described here is to identify quantitative trait loci (QTL) linked to variations in brain anatomy using markers from a genetic map that has been generated from the colony (Jasinska et al., 2007). The pedigree of the colony is well documented, and DNA is available for all of the animals that have been scanned. In related work detailed elsewhere (Fears et al., 2009), it has been demonstrated that the volumes of the brain, cerebellum, and hippocampus and the cross sectional area of the corpus callosum derived from the MRI data are all highly heritable phenotypes; the atlas described here will help in future efforts to define more anatomically restricted phenotypes bounded by identifiable sulcal landmarks. Individuals in the Vervet Research Colony have also been phenotyped for a variety of behavioral traits (Fairbanks et al., 2004a; 2004b), including cognitive phenotypes that have well characterized underlying neural correlates such as working memory (James et al., 2007), and phenotyping of cerebrospinal fluid metabolites has already led to identification of an associated QTL (Freimer et al., 2007). As more anatomically restricted phenotypes are derived from the MRI data, it will be possible to look in detail at relationships between structural, biochemical, functional genomic (Jasinska et al., 2009) and behavioral phenotypes in the vervet. The resulting findings should ultimately help to identify genetic and environmental underpinnings of human brain anatomy and behavior.

Acknowledgments

The support of Jeff Alger, Robert Bilder, David Jentsch, John Mazziotta and Peter Whybrow is gratefully acknowledged. Members of the VRC management and MRI scanning team included Kelli Barnet, Stephanie Groman, Jennifer Kay and Glenville Morton. Scott Fears was supported by the Training Grant for Neurobehavioral Genetics, 5T32NS048004. Funding was provided by the NIH Roadmap for Biomedical Research, Grant U54 RR021813; the UCLA Semel Institute; NCRR 2R01RR016300-03; P40RR019963 and 5P20RR020750-03. Supported was also provided by Grant Numbers RR12169, RR13642 and RR00865 from the National Center for Research Resources (NCRR), a component of the National Institutes of Health (NIH). Acquisition of the cryomacrotome data was supported in part by the United States Department of Energy contract DE-FC03-87-ER60615.

For generous support the authors also wish to thank the Brain Mapping Medical Research Organization, Brain Mapping Support Foundation, Pierson-Lovelace Foundation, The Ahmanson Foundation, William M. and Linda R. Dietel Philanthropic Fund at the Northern Piedmont Community Foundation, Tamkin Foundation, Jennifer Jones-Simon Foundation, Capital Group Companies Charitable Foundation, Robson Family and Northstar Fund.

Abbreviations

AIR	Automated Image Registration
CIE	International Commission on Illumination
DICOM	Digital Imaging and Communications in Medicine file format
JPEG	Joint Photographic Experts Group file format
MRI	Magnetic Resonance Imaging
NIfTI	Neuroimaging Informatics Technology Initiative file format
PNG	Portable Network Graphic file format
ppm	portable pixmap file format
QTL	Quantitative Trait Loci
SVG	Scalable Vector Graphics
TE	excitation time
TI	inversion time
TR	repetition time
UCLA	University of California, Los Angeles
URL	Uniform Resource Locator
VA	Veterans Administration

References

Annese, J.; Toga, AW. Postmortem anatomy. In: Toga, AW.; Mazziotta, JC., editors. Brain Mapping: The Methods. Second Edition. Academic Press; Boston: 2002. p. 537-571.

Bailey JN, Breidenthal SE, Jorgensen MJ, McCracken JT, Fairbanks LA. The association of DRD4 and novelty seeking is found in a nonhuman primate model. Psychiatr. Genet 2007;17:23–27. [PubMed: 17167341]

Black KJ, Snyder AZ, Koller JM, Gado MH, Perlmutter JS. Template images for nonhuman primate neuroimaging: 1. Baboon. Neuroimage 2001a;14:736–743. [PubMed: 11506545]

Black KJ, Koller JM, Snyder AZ, Perlmutter JS. Template images for nonhuman primate neuroimaging: 2. Macaque. Neuroimage 2001b;14:744–748. [PubMed: 11506546]

Black KJ, Koller JM, Perlmutter JS. Template images for neuroimaging in Macaca fascicularis, 2005. Neuroscience Meeting Planner. 2005 Program No. 454.18.

Brodmann, K. Vergleichende Lokalisationslehre der Grosshirnrinde in ihren Prinzipien dargestellt auf Grund des Zellenbaues. Barth; Leipzig: 1909.

Burke MW, Palmour RM, Ervin FR, Ptito M. Neuronal reduction in frontal cortex of primates after prenatal alcohol exposure. Neuroreport 2009;20:13–17. [PubMed: 18987558]

Burke MW, Zangenehpour S, Ptito M. Partial recovery of hemiparesis following hemispherectomy in infant monkeys. Neurosci. Lett 2010;469:243–247. [PubMed: 19969043]

Campos-Romo A, Ojeda-Flores R, Moreno-Briseño P, Fernandez-Ruiz J. Quantitative evaluation of MPTP-treated nonhuman parkinsonian primates in the HALLWAY task. J. Neurosci. Methods 2009;177:361–368. [PubMed: 19022292]

Cannestra AF, Santori EM, Holmes CJ, Toga AW. A three-dimensional multimodality brain map of the nemestrina monkey. Brain. Res. Bull 1997;43:141–148. [PubMed: 9222526]

Carlsson HE, Schapiro SJ, Farah I, Hau J. Use of primates in research: a global overview. Am. J. Primatol 2004;63:225–237. [PubMed: 15300710]

Chakravarty, MM.; Frey, S.; Collins, DL. Digital atlas of the rhesus monkey brain in stereotaxic coordinates. In: Paxinos, G.; Huang, XF.; Petrides, M.; Toga, AW., editors. The Rhesus Monkey Brain in Stereotaxic Coordinates. Academic Press; San Diego, CA: 2009. p. 403-407.

Cline D, Jeschke S, White K, Razdan A, Wonka P. Dart throwing on surfaces. Comput. Graph. Forum 2009;28:1217–1226.

Connolly CJ. The fissural patterns of the primate brain. Am. J. Phys. Anthropol 1936;21:301–422.

Contreras CM, Mexicano G, Guzman-Flores C. A stereotaxic brain atlas of the green monkey (Cercopithecus aethiops aethiops). Bol. Estud. Med. Biol 1981;31:383–428. [PubMed: 6751347]

Elmore D, Eberle R. Monkey B virus (Cercopithecine herpesvirus 1). Comp. Med 2008;58:11–21. [PubMed: 19793452]

Ervin FR, Palmour RM, Young SN, Guzman-Flores C, Juarez J. Voluntary consumption of beverage alcohol by vervet monkeys: population screening, descriptive behavior and biochemical measures. Pharmacol. Biochem. Behav 1990;36:367–373. [PubMed: 2356209]

Fainman J, Eid MD, Ervin FR, Palmour RM. A primate model for Alzheimer's disease: investigation of the apolipoprotein E profile of the vervet monkey of St. Kitts. Am. J. Med. Genet. B. Neuropsychiatr. Genet 2007;144B:818–819. [PubMed: 17373728]

Fairbanks LA, Jorgensen MJ, Huff A, Blau K, Hung YY, Mann JJ. Adolescent impulsivity predicts adult dominance attainment in male vervet monkeys. Am. J. Primatol 2004a;64:1–17. [PubMed: 15356854]

Fairbanks LA, Newman TK, Bailey JN, Jorgensen MJ, Breidenthal SE, Ophoff RA, Comuzzie AG, Martin LJ, Rogers J. Genetic contributions to social impulsivity and aggressiveness in vervet monkeys. Biol. Psychiatry 2004b;55:642–647. [PubMed: 15013834]

Falk D. Brain evolution in Old World monkeys. Am. J. Phys. Anthropol 1978;48:315–320. [PubMed: 416723]

Fears SC, Melega WP, Service SK, Lee C, Chen K, Tu Z, Jorgensen MJ, Fairbanks LA, Cantor RM, Freimer NB, et al. Identifying heritable brain phenotypes in an extended pedigree of vervet monkeys. J. Neurosci 2009;29:2867–2875. [PubMed: 19261882]

Freimer NB, Service SK, Ophoff RA, Jasinska AJ, McKee K, Villeneuve A, Belisle A, Bailey JN, Breidenthal SE, Jorgensen MJ, et al. A quantitative trait locus for variation in dopamine metabolism mapped in a primate model using reference sequences from related species. Proc. Natl. Acad. Sci. U. S. A 2007;104:15811–15816. [PubMed: 17884980]

Gil-da-Costa R, Hauser MD. Vervet monkeys and humans show brain asymmetries for processing conspecific vocalizations, but with opposite patterns of laterality. Proc. Biol. Sci 2006;273:2313–2318. [PubMed: 16928633]

Greer PJ, Villemagne VL, Ruszkiewicz J, Graves AK, Meltzer CC, Mathis CA, Price JC. MR atlas of the baboon brain for functional neuroimaging. Brain. Res. Bull 2002;58:429–438. [PubMed: 12183022]

Groves, CP. Primate taxonomy. Washington, DC; Smithsonian Institution Press: 2001.

Grubb P, Butynski TM, Oates JF, Bearder SK, Disotell TR, Groves CP, Struhsaker TT. Assessment of the diversity of African primates. Int. J. Primatol 2003;24:1301–1357.

Guennebaud G, Germann M, Gross M. Dynamic sampling and rendering of algebraic point set surfaces. Comput. Graph. Forum 2008;27:653–662.

Hugo C, Seier J, Mdhluli C, Daniels W, Harvey BH, Du Toit D, Wolfe-Coote S, Nel D, Stein DJ. Fluoxetine decreases stereotypic behavior in primates. Prog. Neuropsychopharmacol. Biol. Psychiatry 2003;27:639–643. [PubMed: 12787851]

James AS, Groman SM, Seu E, Jorgensen M, Fairbanks LA, Jentsch JD. Dimensions of impulsivity are associated with poor spatial working memory performance in monkeys. J. Neurosci 2007;27:14358–14364. [PubMed: 18160643]

Jasinska AJ, Service S, Levinson M, Slaten E, Lee O, Sobel E, Fairbanks LA, Bailey JN, Jorgensen MJ, Breidenthal SE, et al. A genetic linkage map of the vervet monkey (Chlorocebus aethiops sabaeus). Mamm. Genome 2007;18:347–360. [PubMed: 17629771]

Jasinska AJ, Service S, Choi OW, DeYoung J, Grujic O, Kong SY, Jorgensen MJ, Bailey J, Breidenthal S, Fairbanks LA, et al. Identification of brain transcriptional variation reproduced in peripheral blood: an approach for mapping brain expression traits. Hum. Mol. Genet 2009;18:4415–4427. [PubMed: 19692348]

Jentsch JD, Redmond DE, Elsworth JD, Taylor JR, Youngren KD, Roth RH. Enduring cognitive deficits and cortical dopamine dysfunction in monkeys after long-term administration of phencyclidine. Science 1997;277:953–955. [PubMed: 9252326]

Jentsch JD, Olausson P, De La Garza R, Taylor JR. Impairments of reversal learning and response perseveration after repeated, intermittent cocaine administrations to monkeys. Neuropsychopharmacology 2002;26:183–190. [PubMed: 11790514]

Laćan G, De Salles AA, Gorgulho AA, Krahl SE, Frighetto L, Behnke EJ, Melega WP. Modulation of food intake following deep brain stimulation of the ventromedial hypothalamus in the vervet monkey. Laboratory investigation. J. Neurosurg 2008;108:336–342. [PubMed: 18240931]

Lemere CA, Beierschmitt A, Iglesias M, Spooner ET, Bloom JK, Leverone JF, Zheng JB, Seabrook TJ, Louard D, Li D, et al. Alzheimer's disease abeta vaccine reduces central nervous system abeta levels in a non-human primate, the Caribbean vervet. Am. J. Pathol 2004;165:283–297. [PubMed: 15215183]

Likar B, Viergever MA, Pernus F. Retrospective correction of MR intensity inhomogeneity by information minimization. IEEE. Trans. Med. Imaging 2001;20:1398–1410. [PubMed: 11811839]

Marais L, Daniels W, Brand L, Viljoen F, Hugo C, Stein DJ. Psychopharmacology of maternal separation anxiety in vervet monkeys. Metab. Brain. Dis 2006;21:201–210. [PubMed: 16850260]

Mash DC, Staley JK, Doepel FM, Young SN, Ervin FR, Palmour RM. Altered dopamine transporter densities in alcohol-preferring vervet monkeys. Neuroreport 1996;7:457–462. [PubMed: 8730805]

Mazziotta J, Toga A, Evans A, Fox P, Lancaster J, Zilles K, Woods R, Paus T, Simpson G, Pike B, et al. A probabilistic atlas and reference system for the human brain: International Consortium for Brain Mapping (ICBM). Philos. Trans. R. Soc. Lond. B. Biol. Sci 2001;356:1293–1322. [PubMed: 11545704]

McLaren DG, Kosmatka KJ, Oakes TR, Kroenke CD, Kohama SG, Matochik JA, Ingram DK, Johnson SC. A population-average MRI-based atlas collection of the rhesus macaque. Neuroimage 2009;45:52–59. [PubMed: 19059346]

Melega WP, Laćan G, Harvey DC, Way BM. Methamphetamine increases basal ganglia iron to levels observed in aging. Neuroreport 2007;18:1741–1745. [PubMed: 17921879]

Melega WP, Jorgensen MJ, Laćan G, Way BM, Pham J, Morton G, Cho AK, Fairbanks LA. Long-term methamphetamine administration in the vervet monkey models aspects of a human exposure: brain neurotoxicity and behavioral profiles. Neuropsychopharmacology 2008;33:1441–1452. [PubMed: 17625500]

Mikula S, Trotts I, Stone JM, Jones EG. Internet-enabled high-resolution brain mapping and virtual microscopy. Neuroimage 2007;35:9–15. [PubMed: 17229579]

Ouwe-Missi-Oukem-Boyer O, Mezui-Me-Ndong J, Boda C, Lamine I, Labrousse F, Bisser S, Bouteille B. The vervet monkey (Chlorocebus aethiops) as an experimental model for Trypanosoma brucei gambiense human African trypanosomiasis: a clinical, biological and pathological study. Trans. R. Soc. Trop. Med. Hyg 2006;100:427–436. [PubMed: 16325877]

Paxinos, G.; Huang, XF.; Petrides, M.; Toga, AW. The Rhesus Monkey Brain in Stereotaxic Coordinates. Second Edition. Academic Press; San Diego, CA: 2009.

Rubins DJ, Ambach K, Toga AW, Melega WP, Cherry SR. Development of a digital brain atlas of the vervet monkey. J. Cereb. Blood. Flow. Metab 1999;19(suppl):S781.

Saleem, KS.; Logothetis, N. A combined MRI and histology atlas of the rhesus monkey brain in stereotaxic coordinates. Academic; Burlington, MA: 2007.

Steiper ME, Young NM. Primate molecular divergence dates. Mol. Phylogenet. Evol 2006;41:384–394. [PubMed: 16815047]

Stewart CB, Disotell TR. Primate evolution - in and out of Africa. Curr. Biol 1998;8:R582–R588. [PubMed: 9707399]

Taylor JR, Elsworth JD, Roth RH, Sladek JR, Redmond DE. Severe long-term 1-methyl-4-phenyl-1,2,3,6-tetrahydropyridine-induced parkinsonism in the vervet monkey (Cercopithecus aethiops sabaeus). Neuroscience 1997;81:745–755. [PubMed: 9316026]

Tosi AJ, Disotell TR, Morales JC, Melnick DJ. Cercopithecine Y-chromosome data provide a test of competing morphological evolutionary hypotheses. Mol. Phylogenet. Evol 2003;27:510–521. [PubMed: 12742755]

Tosi AJ, Detwiler KM, Disotell TR. X-chromosomal window into the evolutionary history of the guenons (Primates: Cercopithecini). Mol. Phylogenet. Evol 2005;36:58–66. [PubMed: 15904856]

Uno H, Tarara R, Else JG, Suleman MA, Sapolsky RM. Hippocampal damage associated with prolonged and fatal stress in primates. J. Neurosci 1989;9:1705–1711. [PubMed: 2723746]

Van Der Gucht E, Youakim M, Arckens L, Hof PR, Baizer JS. Variations in the structure of the prelunate gyrus in Old World monkeys. Anat. Rec. A. Discov. Mol. Cell. Evol. Biol 2006;288:753–775. [PubMed: 16779809]

van der Kuyl AC, Dekker JT, Goudsmit J. St. Kitts green monkeys originate from West Africa: Genetic evidence from feces. Am. J. Primatol 1996;40:361–364.

Vogt C, Vogt O. Allgemeinere Ergebnisse unsere Hirnforschung. Journal für Psychologie und Neurologie 1919;25:279–462.

von Bonin, G.; Bailey, P. The neocortex of Macaca mulatta. University of Illinois Press; Urbana: 1947.

Woods RP, Grafton ST, Holmes CJ, Cherry SR, Mazziotta JC. Automated image registration: I. General methods and intrasubject, intramodality validation. J. Comput. Assist. Tomogr 1998a; 22:139–152. [PubMed: 9448779]

Woods RP, Grafton ST, Watson JD, Sicotte NL, Mazziotta JC. Automated image registration: II. Intersubject validation of linear and nonlinear models. J. Comput. Assist. Tomogr 1998b;22:153–165. [PubMed: 9448780]

Woods RP. Characterizing volume and surface deformations in an atlas framework: theory, applications, and implementation. Neuroimage 2003a;18:769–788. [PubMed: 12667854]

Woods RP. Multitracer: a Java-based tool for anatomic delineation of grayscale volumetric images. Neuroimage 2003b;19:1829–1834. [PubMed: 12948737]

Xing J, Wang H, Zhang Y, Ray DA, Tosi AJ, Disotell TR, Batzer MA. A mobile element-based evolutionary history of guenons (tribe Cercopithecini). BMC. Biol 2007;5:5. [PubMed: 17266768]

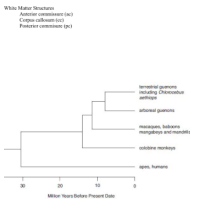

Figure 1.
Relationship of *Chlorocebus aethiops* to other Old World monkeys, apes and humans. Estimated divergence dates are represented along the x-axis.

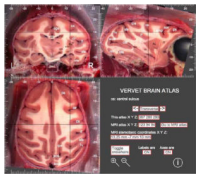

Figure 2.

A view from the cryomacrotome atlas at the gray-white interface near the floor of the central sulcus. Views can be adjusted by clicking on the images, by using the buttons labeled `<-' and`->', by clicking on one of the coordinate buttons and modifying the displayed values or by selecting an anatomic structure from one of the pull-down menus (not shown). Stereotaxic coordinates in the space defined by the averaged MRI atlas are displayed and can be modified by clicking on the coordinates. Anatomic labels, coordinate axes and crosshairs can be turned on and off using buttons near the bottom of the control panel. The view can be magnified or minified by pressing the corresponding icon. The “Go to MRI atlas” button generates the view of the averaged MRI atlas illustrated in Figure 4. See Table 1 for full names and abbreviations of structures.

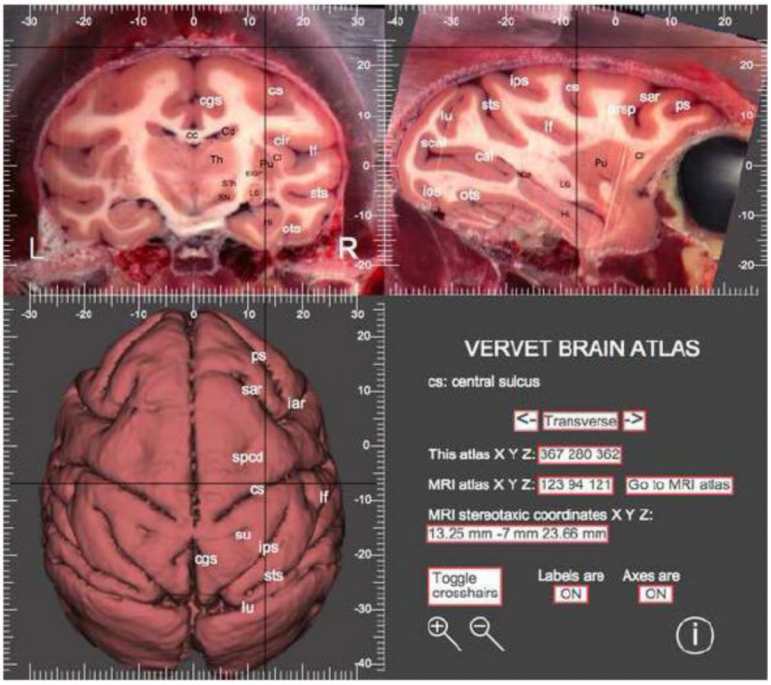

Figure 3.

A view from the cryomacrotome atlas with a surface rendered transverse view. Clicking on the images well outside the brain in the cryomacrotome atlas displays a surface rendered view rather than a slice with no visible brain tissue. See Figure 2 legend for additional information.

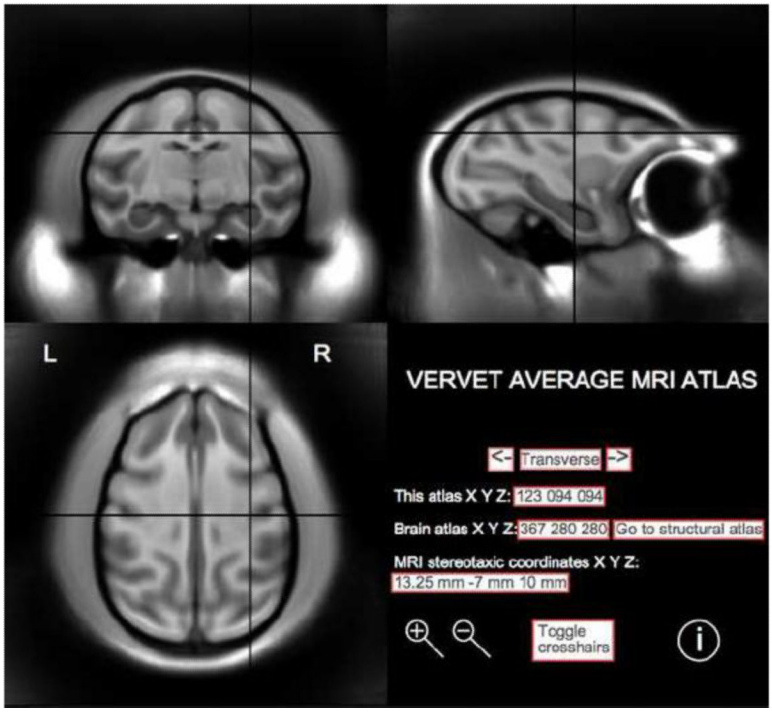

Figure 4.
A view from the averaged MRI atlas corresponding the cryomacrotome atlas shown in Figure 2. Navigation to other views is analogous to that in the cryomacrotome atlas. The "Go to structural atlas" generates the cryomacrotome atlas view illustrated in Figure 2.

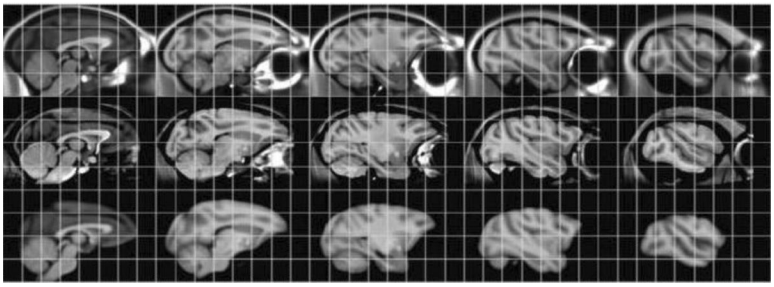

Figure 5.
Sagittal slices from the vervet MRI atlas (first row), from the MNI rhesus macaque MRI atlas (Chakravarty et al., 2009) (second row) and from the 112RM-SL T1-weighted rhesus macaque atlas (McLaren et al., 2009) (third row). The images from the latter two atlases have been resampled into the vervet MRI atlas spaces. Slices in the five columns correspond to X=0.25mm, 5.25 mm, 10.25 mm, 15.25 mm and 20.25 mm in the atlas. The superimposed grid lines are at the same stereotaxic locations in all three rows.

Table 1

Anatomic landmarks labeled in the cryomacrotome atlas

Sulcal landmarks
Anterior middle temporal sulcus (amt)
Anterior supraprincipal dimple (aspd)
Arcuate sulcus spur (arsp)
Anterior subcentral dimple (asd)
Calcarine sulcus (cal)
Central sulcus (cs
Cingulate sulcus (cgs)
Circular sulcus (cir)
Hippocampal fissure (hf)
Inferior arcuate sulcus (iar)
Inferior calcarine sulcus (ical)
Inferior occipital sulcus (ios)
Intraparietal sulcus (ips)
Lateral orbital sulcus (lorb)
Lateral fissure (lf)
Lunate sulcus (lu)
Medial orbital sulcus (morb)
Occipitotemporal sulcus (ots)
Parietooccipital sulcus (pos
Posterior middle temporal sulcus (pmt)
Principal sulcus (ps)
Rhinal fissure (rf)
Rostral sulcus (ros)
Superior arcuate sulcus (sar)
Superior calcarine sulcus (scal)
Superior postcentral dimple (su)
Superior precentral dimple (spcd
Superior temporal sulcus (sts)
Gray Matter Structures
Amygdala (Amy)
Caudate nucleus (Cd)
Claustrum (Cl)
External globus pallidus (EGP)
Hippocampus (Hi)
Hypothalamus (Hy)
Nucleus Accumbens (Acb)
Internal globus pallidus (IGP)
Lateral geniculate (LG)
Putamen (Pu)

Substantia nigra (SN)
Subthalamic nucleus (STh)
Thalamus (Th)
White Matter Structures
Anterior commissure (ac)
Corpus callosum (cc)
Posterior commisure (pc)